Journal of Structural Biology 191 (2015) 190–196

Contents lists available at ScienceDirect

Journal of Structural Biology

journal homepage: www.elsevier.com/locate/yjsbi

3D reconstruction of SEM images by use of optical photogrammetry software

Mona Eulitz *, Gebhard Reiss

Institute for Anatomy and Clinical Morphology, School of Medicine, Faculty of Health, Witten/Herdecke University, Alfred-Herrhausen-Straße 50, D-58448 Witten, Germany

ARTICLE INFO

Article history:
Received 26 February 2015
Received in revised form 6 June 2015
Accepted 11 June 2015
Available online 11 June 2015

Keywords:
3D surface reconstruction
Mesh
Photogrammetry
Point cloud
Scanning Electron Microscopy
Surface morphology

ABSTRACT

Reconstruction of the three-dimensional (3D) surface of an object to be examined is widely used for structure analysis in science and many biological questions require information about their true 3D structure. For Scanning Electron Microscopy (SEM) there has been no efficient non-destructive solution for reconstruction of the surface morphology to date. The well-known method of recording stereo pair images generates a 3D stereoscope reconstruction of a section, but not of the complete sample surface.

We present a simple and non-destructive method of 3D surface reconstruction from SEM samples based on the principles of optical close range photogrammetry. In optical close range photogrammetry a series of overlapping photos is used to generate a 3D model of the surface of an object. We adapted this method to the special SEM requirements. Instead of moving a detector around the object, the object itself was rotated. A series of overlapping photos was stitched and converted into a 3D model using the software commonly used for optical photogrammetry. A rabbit kidney glomerulus was used to demonstrate the workflow of this adaption. The reconstruction produced a realistic and high-resolution 3D mesh model of the glomerular surface.

The study showed that SEM micrographs are suitable for 3D reconstruction by optical photogrammetry. This new approach is a simple and useful method of 3D surface reconstruction and suitable for various applications in research and teaching.

1. Introduction

3D reconstruction is an essential tool for structure analysis, and SEM is a versatile tool to examine small samples. It is widely used for imaging and analysis in different fields of research and technical industry (Jensen, 2012; Sun and Xia, 2002). The sample size is limited by the specimen chamber and differs between various standard SEM (Klein and Romero, 2007).

In SEM, a focused electron beam scans the surface of the sample. The electrons interact with atoms of the surface and a detector picks up the signal generated by interaction of the beam with the surface. Various signals can be detected containing information about the sample surface topography and composition (Egerton, 2005). Maximum magnification is about 100,000× (Everhart and Hayes, 1972).

The prevalent detection mode is the detection of secondary electrons (SE). Interaction of the electrons with the surface results in emission of SE with lower energy (Egerton, 2005; Reimer, 2013). Their emission depends on type and orientation of the surface. Emitted SE are registered by a detector, amplified and finally visualized as a two-dimensional micrograph of the 3D sample with a large depth of field (Egerton, 2005). The resulting 2D micrograph contains topographic information that characteristically resembles obliquely illuminated solid objects. Although a large portion of the sample is in focus and the micrograph possess a 3D appearance, it is only 2D. Nevertheless, 3D data of the sample morphology are often essential. It was the aim of the present study to develop a new, non-invasive and uncomplicated method of 3D reconstruction of the sample surface, based on optical close-range photogrammetry.

Optical close-range photogrammetry has become popular in recent years due to the availability of suitable digital cameras, low-cost software, and an easy to use digital workflow. Photogrammetry plays, for example, an important role in archaeological research (Lambers and Remondino, 2008). 3D surface reconstruction quality is constantly improving in optical close-range photogrammetry. Even simple inexpensive smartphone cameras are suited for scientific 3D reconstruction studies (Bakuła and Flasiński, 2014).

* Corresponding author.
E-mail addresses: mona.eulitz@uni-wh.de (M. Eulitz), greiss@uni-wh.de (G. Reiss).

http://dx.doi.org/10.1016/j.jsb.2015.06.010
1047-8477/

Advantages of this new method are the low additional technical efforts and the non-destruction of the examined sample. In optical photography, close-range photogrammetry is a well-known method of producing 3D models from series of overlapping images of an object. Series of images are taken from different locations around the object. Every object point to be converted in 3D has to be recorded by at least two different images (Luhmann et al., 2013). Images are taken around the object and well established software programs are used to stitch the overlapping images to generate a 3D mesh model (Fig. 1a). A number of popular free or low-cost programs are available today (Bemis et al., 2014).

The final 3D mesh model of the sample surface can be rotated, viewed from all angles and at variable magnification. The 3D mesh model of the surface allows measurement and capture of shape, size and volume (Yakar and Yilmaz, 2008). Another advantage of the virtual 3D mesh model is that it is also possible to convert the mesh surface into a volume model and to print a 3D model of the surface (Partridge et al., 2012; Schilling et al., 2014).

In the present paper we investigated the possibility of transferring this technique of optical close-range photogrammetry to the special features of SEM. Instead of moving the fixed SE detector, the sample was rotated. The sample fastened to a rotatable stage in the SEM chamber was rotated in small steps around its own axis (Fig. 1b).

2. Materials and methods

2.1. Sample preparation and SEM

A glomerulus in the cortex of an already existing rabbit kidney sample was used as a test specimen. Animal care and treatment was conducted in conformity with the German law of animal protection. The sample was treated as follows: small sections of the kidney (approx. $5 \times 5 \times 5$ mm) were perfused with fixative (3% glutaraldehyde, buffered with 0.1 M sodium cacodylate buffer, pH 7.4) and postfixed with a combination of osmium tetroxide and thiocarbohydrazide (TCH, OTOTO-method adaption from Seligman et al. (1966)). The samples were dehydrated in a graded acetone series, rinsed with liquid CO_2 and critical point dried. Dried specimens were mounted onto metal stubs with carbon-coated tabs. No additional sputtering was necessary since each sample was stabilized by OTOTO treatment (conductivity and stability enhancement).

SEM was performed on a Sigma VP (Zeiss, Oberkochen, Germany) scanning electron microscope using the SE detector with an acceleration voltage of 5 kV, in high vacuum mode, 8 mm working distance, 2720× magnification, 30 µm aperture, 1.5 nm spot size and a pixel dwell time of 25.6 µs. Electrons were emitted by a field electron gun and the Everhart–Thornley Detector was used as secondary electron detector. Each micrograph was focussed manually, and manual stigmator correction was applied after every tenth micrograph.

2.2. Hardware and software equipment

A quad-core core Intel i7-4770K CPU desktop with 32 GB of RAM, GeForce GTX 760 video card and 64-bit operating system (Windows 7) was used for image processing and reconstruction. Micrographs were taken with the Zeiss SmartSEM software (Zeiss, Oberkochen, Germany version 05.00). The software program GIMP (version 2.8.4) was used for manual image processing (alignment of brightness and contrast between the photos). There are several programs which can be used for the reconstruction of 3D mesh models from series of overlapping images in optical photogrammetry. We used three of the most popular software programs: 123D Catch (Autodesk, USA, cloud computing, version 2.2.3), PhotoScan (Agisoft, St. Petersburg, Russia, version 1.0.4) and Recap 360 Photo (Autodesk, USA, cloud computing, version year 2014).

For high quality calculating of 40 SEM micrographs with local computing (PhotoScan), total time to micrograph alignment took about 10–15 min, dense point cloud calculating 30–40 min and mesh generating 2–5 min. With cloud computing, the whole process took 30–120 min.

The free software Meshmixer (Autodesk, USA, version 2.1) and the beta software Memento (Autodesk, USA, version 1.0.8), free at time of use and particularly suitable for very large mesh vertices (>1,000,000), were used to post process the generated 3D model, fix holes in the 3D mesh and trim margins. Finally, the free software Blender (Blender Foundation, Netherlands, version 2.69) was used to add depth to the mesh model for 3D printing.

2.3. Capture of overlapping SEM micrographs

Micrographs were captured with the SE detector from an exposed glomerulus hemisphere visible on the surface of the kidney fragment.

SEM micrographs were taken manually. For this reason, we decided to take 40 micrographs (in steps of 9°) as a compromise between quality and effort. In optical close range photogrammetry a large overlap between consecutive images allows a reduction of the perspective differences and thus yields better matching results, limiting the number of outliers (Barazzetti et al., 2011). The commonly used overlap between consecutive images is around 80% (Dall'Asta et al., 2015).

The glomerulus was rotated in 40 steps (Fig. 1b) and a single micrograph was captured after each step. A capillary loop in the

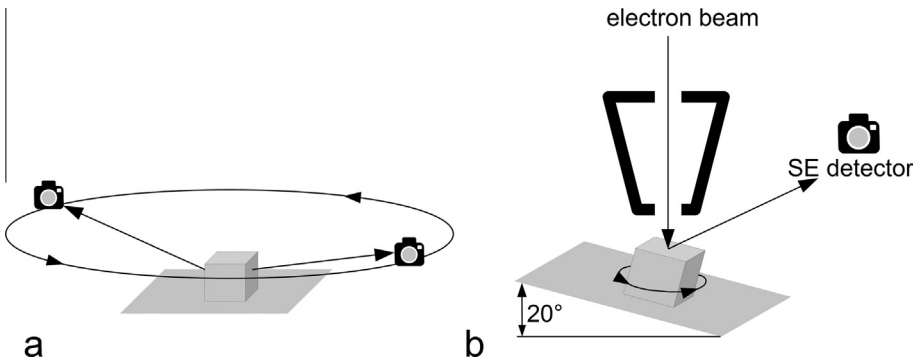

Fig. 1. Adaption of optical photogrammetry. (a) For optical close range photogrammetry, a camera is rotated around the object and overlapping photos are taken. (b) Adaption of this method to the specific characteristics of SEM. The object itself is rotated and overlapping photos are taken by a detector. The object is slightly tilted.

center of the glomerulus, highly visible from all sides, was used as axis of revolution. The capillary loop was centered in each micrograph with the help of a superimposed crosshair (graticule licence, Zeiss SmartSEM software). The overlap between neighboring micrographs achieved a maximum of 97.5%. Depending on the topography of the sample, the actual overlap was somewhat smaller in some cases. Deeper situated structures were overshadowed by higher situated parts and the electron beam was blocked. However, directly adjacent micrographs were very similar caused by large overlapping areas. SEM micrographs with a pixel size about 31 nm were taken manually. At 2720× primary magnification, almost the entire micrograph was filled with an image of the glomerulus. Maximum pixel resolution of the Zeiss SEM scan generator (3072 × 2304) was used and micrographs were saved in the lossless TIF file format. The micrographs were adapted manually in contrast and brightness with GIMP and exported at maximum quality in JPEG file format. JPEG is the common format handled by all tested photogrammetry software programs. Two blurred micrographs caused by mistakes during the manual micrograph acquisition were not used for further processing.

2.4. Workflow and manual stitching

Workflow of SEM photogrammetry is not very different from the workflow of optical photogrammetry (Fig. 2). One difference is certainly that optical 3D reconstruction photogrammetry software was not originally developed for SEM. Photogrammetry software uses metadata in the exchangeable image file format (Exif) stored within the commonly used JPEG file format. Exif data are generated by the optical digital camera. They include, among other less important details, also some useful information about focal length and about the specific camera model (Tesic, 2005). The metadata given in the Zeiss image files cannot provide any useful information for the photogrammetry software. Generation of SEM micrographs is based on a completely different principle and information about focal length is not available.

Photos were processed by all three software programs as if made by an optical camera moving in a circle around an immobile object. All tested programs were robust enough to calculate a 3D model, also without any Exif data.

Reconstruction of the virtual circle was not always accurate. Some photos were not positioned correctly on the virtual circuit and therefore not in line; the result was a poor 3D reconstruction. To improve the quality of reconstruction, we manually stitched virtual displaced photos to adjacent well-positioned photos within the virtual circuit position (Figs. 2 and 3). Manual stitching was possible with 123D catch (Fig. 3) and Recap 360 Photo (not shown).

2.5. 3D printing

The virtual surface-based 3D model was converted into a volume based model by adding depth to the mere surface mesh with the solidify modifier module in the software program Blender and the well-established 3D-printing technology was used to materialize the glomerulus (Jones, 2012; Partridge et al., 2012). Various printing techniques are commonly used (Gross et al., 2014). We applied a color print technique to reproduce the texture of our model. The textured 3D mesh model was printed in grayscale on a multi-color 3D printer (i.materialise, Belgium). The printing technique is based on drops of liquid colored glue, added by a print head on a thin layer of plaster composite powder. This was repeated layer by layer. The final model was cleaned from spare powder and fixed with glue.

3. Results

3.1. Method transfer

The well-known method of optical close-range photogrammetry is suitable for 3D surface reconstruction of SEM micrographs. Overlapping SEM micrographs were made by rotating a sample

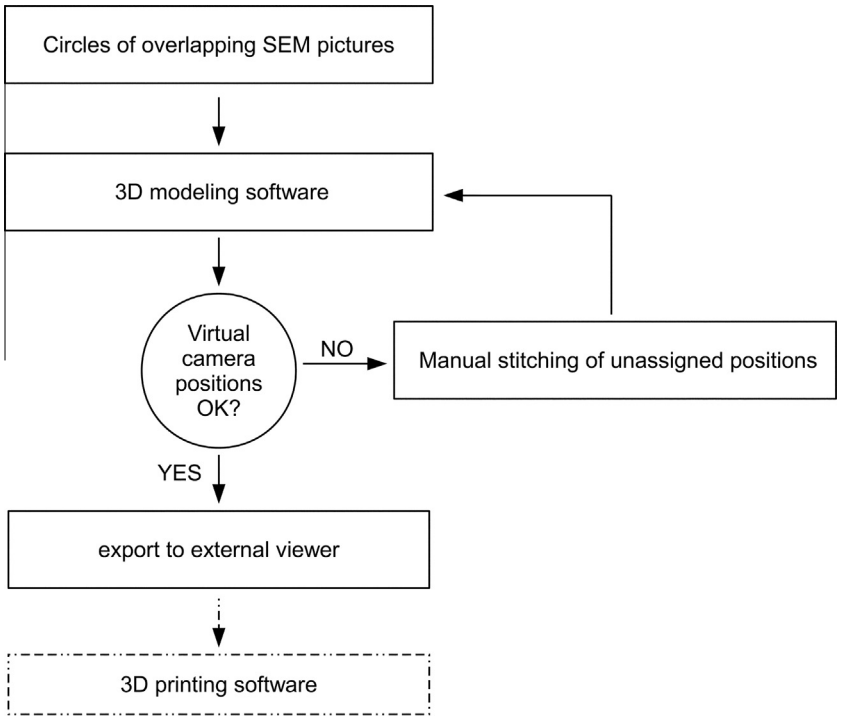

Fig. 2. Workflow of SEM photogrammetry. A group of overlapping photos is processed with standard software for optical photogrammetry. Photos not in appropriate virtual camera positions were manually stitched to adjacent well-positioned photos. The final exported 3D model can be viewed with almost any 3D software.

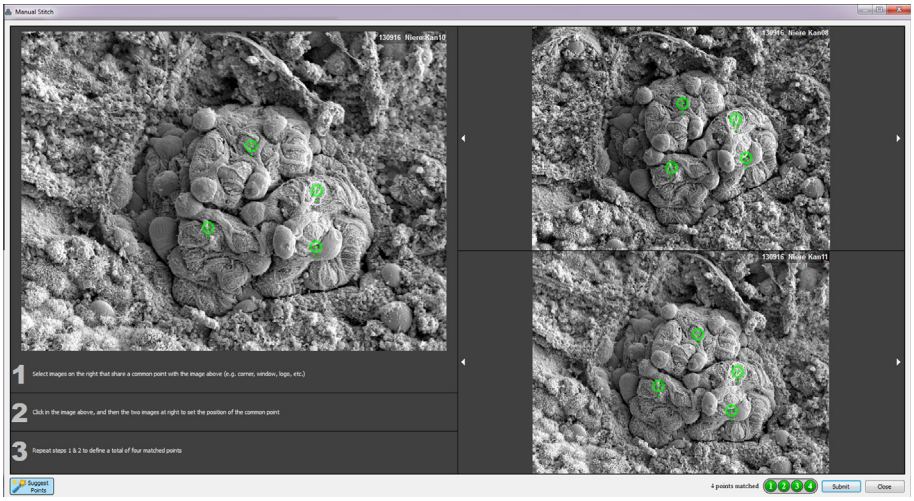

Fig. 3. Example of manual stitching with 123D catch. Four different structures are marked on the displaced SEM micrograph (left) and connected to corresponding positions on two properly oriented photos before (right, top) and after (right, bottom) the displaced photo.

in small steps around its own axis. The sample was slightly tilted (20°) to provide a maximum of surface information. Best quality was achieved by manual stitching of incorrectly positioned virtual camera positions to arrange the photos in an ideal virtual circle (Fig. 4). Blurred photos were deleted (Fig. 4, asterisk).

3.2. Export of surface reconstruction

A point cloud is the first useful result of 3D reconstruction. This is a large collection of data points in a three-dimensional coordinate system to approximate the mean surface of the sample (Fig. 5a and c). Point clouds can be used to get a first impression of the 3D reconstruction and to view the surface topography from all angles. In general, point clouds are not commonly used for final 3D analysis and not all photogrammetry software programs are able to display or export the point clouds. The test calculation, a reconstructed point cloud (in high quality mode), consisted of more than 14 million points (Fig. 5a and c).

In the next step of 3D reconstruction, a mesh model was generated. Point cloud data are used to approximate a triangle mesh of the model surface (Hoppe et al., 1992). A high quality mesh was produced by Recap 360 Photo software in best quality setting (referred to as ultra) (Fig. 5b and d). Vertices (points in a three-dimensional coordinate system with additional information about their color and the direction in which their normal vectors are orientated) are calculated and connected by lines to form a mesh of triangular or polygonal faces. Faces in a common plane form a planar polygon and curved surfaces are approximated by the number of faces. 1,054,400 vertices and 1,042,596 faces were calculated by Recap 360 Photo (Fig. 5b and d). Visible 3D quality is improved by projecting a texture onto the mesh. Shades of gray information in the SEM micrographs are added by the software to

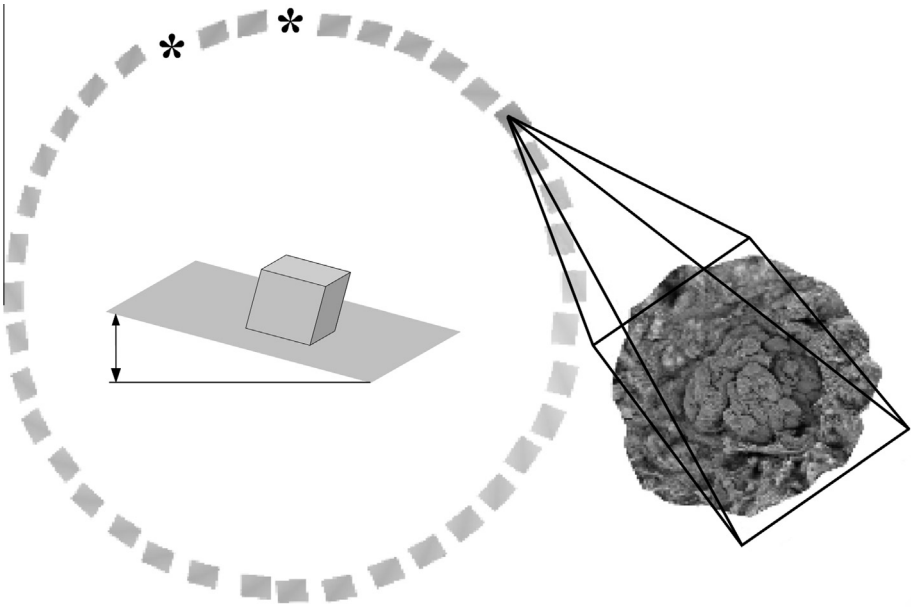

Fig. 4. Circle of virtual camera positions around the sample calculated by Recap 360 Photo after manual stitching. Marked with asterisk are positions of slightly blurred photos which are not used for 3D reconstruction.

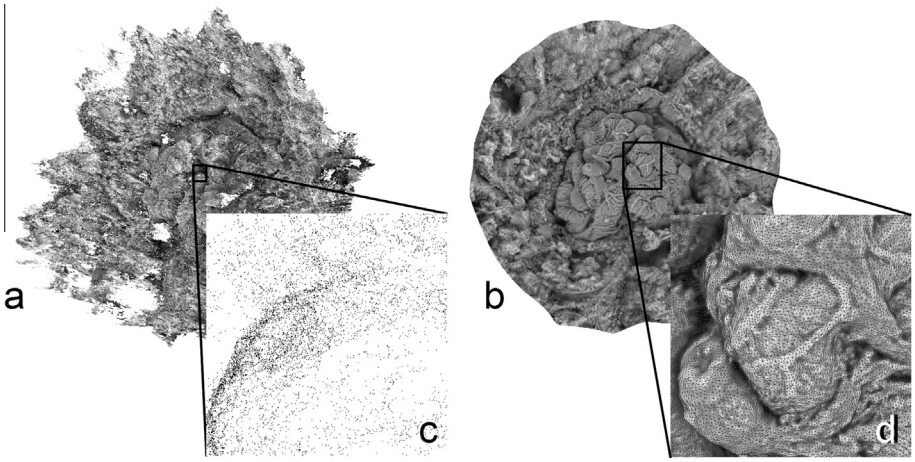

Fig. 5. 3D surface reconstruction. (a) Cloud of points in a three-dimensional coordinate system approximate the mean surface of the sample. (b) Triangle mesh model with added texture. (c and d) Individual points (c) and triangular mesh (d) become visible in the enlargements. ((a), (c) Point cloud calculated by PhotoScan and (b), (d) mesh calculated by Recap 360 Photo.)

generate this mesh texture (Fig. 6b and d). A video to illustrate the 3D surface reconstruction can be found in the Supplement.

3.3. Comparison between 3D reconstruction and SEM micrographs

3D reconstruction of SEM micrographs with optical photogrammetry is an approximation of the original sample surface. Small details, like narrow branches of dentated podocytes (Fig. 6c) are detectable in a 1900×1900 pixel section of the original 3072×2304 pixel original SEM micrograph (Fig. 6a) and can be clearly identified in an enlargement (448×448 pixel) of this section (Fig. 6c). In the 3D reconstruction (Fig. 6b) the same position is zoomed in and a snapshot (354×354 pixel) of a comparable section (Fig. 6d) reveals far poorer edge sharpness.

A comparison between the proportion in the morphology of the glomerulus in the SEM micrographs and in the 3D reconstruction did not reveal any significant difference at a first glance. We selected one SEM micrograph and superimposed it with a corresponding image of the 3D reconstruction. The 3D textured mesh model was orientated in equivalent position, size and with comparable brightness and contrast. Screenshot of the 3D model (Fig. 6f) was subtracted by GIMP from the SEM micrograph (Fig. 6e). 100% coherent photos match should result in a black image. Due to the reduced edge sharpness of the 3D model, contour lines are still visible (Fig. 6g) but no remarkable distortions in the proportion were found.

3.4. Optional 3D printing

A physical model is useful to get a better understanding of the morphology. The 3D print was well-suited to obtain an overall impression of the glomerulus morphology (Fig. 7).

Larger protrusions wind themselves around the blood vessels like the tentacles of an octopus. Shapes of podocytes, their cell bodies and the course of the enveloped blood vessels were highly visible. Detail resolution of the used 3D-printing technique is around 0.8–1.0 mm and leads to a loss of resolution. A large model was printed to keep this loss of quality small, but particularly narrow dentated podocytes protrusions are hardly visible.

4. Discussion

4.1. SEM surface reconstruction by optical photogrammetry

This report demonstrates that the well-established method of optical photogrammetry may be transmitted smoothly and successfully to the particular aspects of SEM images. The OTOTO treated glomerulus was selected because of its complex and detailed surface and availability. A sputter coated SEM sample (data not shown) was also tested and was equally suitable for reconstruction. The only condition for reconstruction is that the sample has to remain stable during the whole electron irradiation time.

Our test, a 3D reconstruction of a kidney glomerulus hemisphere, produced a realistic 3D mesh model of the glomerulus surface, although SEM images exported in JPEG file format do not provide useful Exif metadata. Optical photogrammetry software is robust enough to calculate a 3D mesh in good quality without metadata.

Metadata information can be advantageous for the photogrammetry software, if details about the optical properties (aberrations) of the specific lenses are available (Choi et al., 2006). In an optical system, light is projected through a lens system onto a light sensitive detector (digital sensor), and lens aberrations and focal length have a direct impact on image quality. These data might have a positive influence on the quality of 3D reconstruction (Brown, 1971; Fraser and Al-Ajlouni, 2006).

Micrographs are generated in a somewhat different manner by a SEM. The scanning beam is controlled in a SEM via magnetic lenses (Egerton, 2005). Magnetic lens aberration has no direct effect on the SEM detector and is therefore not comparable with optical lens aberration, the detector reads a signal generated by interaction of the scanning electron beam with the sample surface point by point. However it is conceivable that further adjustments of photogrammetry software might also contribute to improved 3D reconstruction of SEM generated micrographs. One significant advantage of SEM images is their high focus depth compared to photos taken with a conventional photo camera. This might additionally improve the quality of 3D reconstruction.

An alternative method of 3D reconstruction by recording stereo pair images with different tilt angles depends on the accuracy of the tilt angle (Marinello et al., 2008). The drawback of this approach is that 3D reconstruction is limited only to this image

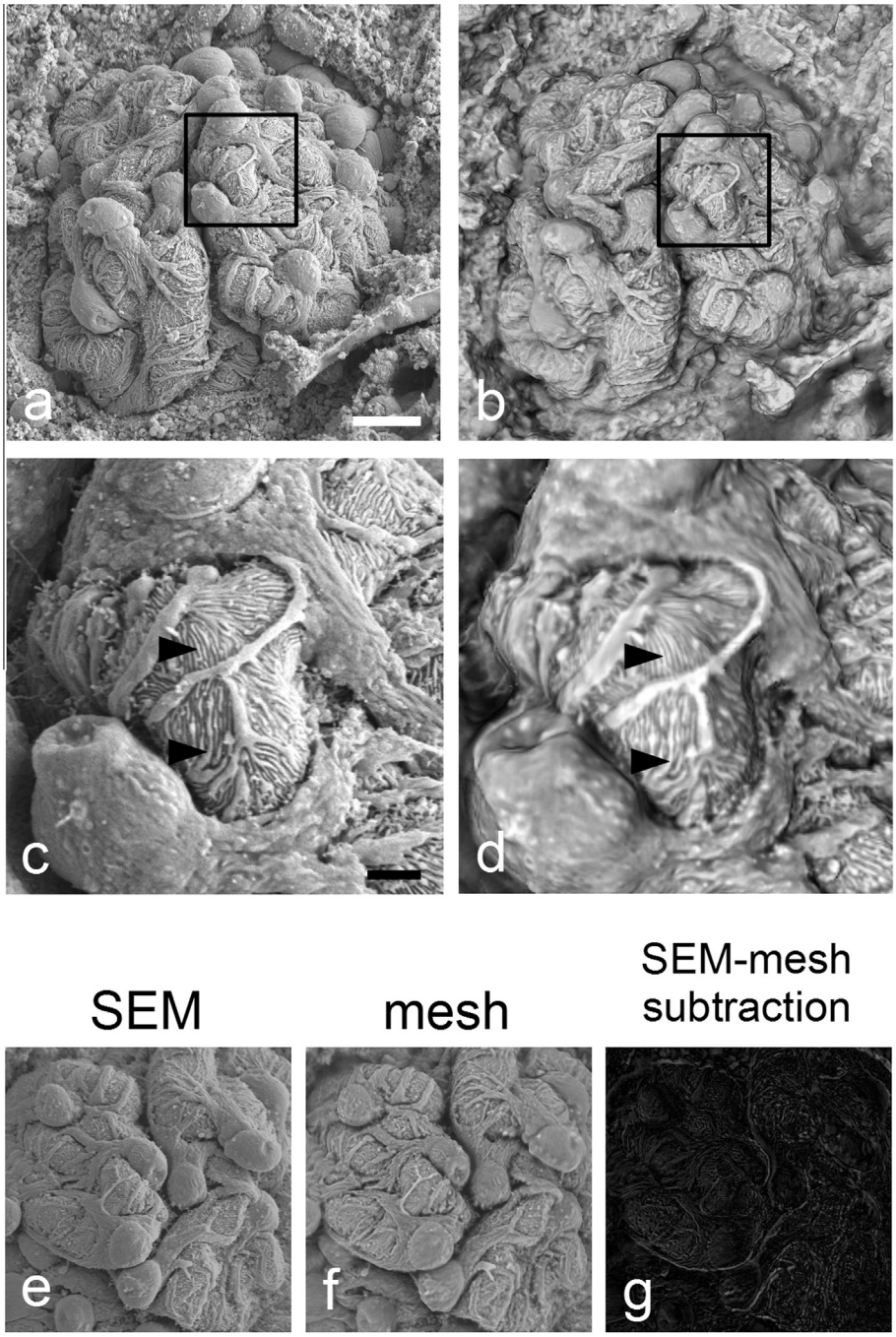

Fig. 6. Comparison between original SEM micrograph (a and c) and screenshot of the textured 3D mesh model rotated to an equivalent position (b and d). (a) Insight into an opened Bowman's Capsule. Blood capillaries are covered with a layer of podocytes. (c) Detail enlargement, dentated cellular protrusions (arrowheads) of the podocytes are clearly visible. 3D model (b) and detail enlargement (d) with comparable detail resolution (arrowheads, dentated protrusions) yet less sharpness of edges. Scale bar, 10 μm (a and b), 2 μm (c and d). (e and f) Comparison between the proportion between SEM (e) and 3D reconstruct (f). Comparable areas arranged in almost equal position are superimposed. Subtraction of congruent grayscale values in (e) and (f) result in black image areas (g).

section. Multiple stereo pair image sets must be made to reconstruct the complete sample surface. In contrast to this complex method, SEM close range photogrammetry is far more simple and does not depend on stereo pair images. Images taken at least every 15° (24 images) are recommended to produce a complete digital model for reconstruction of complex details in which some parts occlude others from many angles (Falkingham, 2012). Any reconstructed point should be presented in five images from different positions, even if those positions differ by only a small amount (To et al., 2015). In order to improve the accuracy of reconstruction in close range photogrammetry, the number of camera views can be increased by moving the camera, or equivalently, by moving the object and taking additional images (Wallace et al., 2005).

We expect the same improvement in quality for future SEM 3D reconstruction. Acquisition of micrographs can be automated and an increase of micrographs seems to be feasible.

4.2. Limitations

Not all SEM objects are suitable for reconstruction by photogrammetry. The sample has to remain stable without deformations during the required time of images acquisition. If the

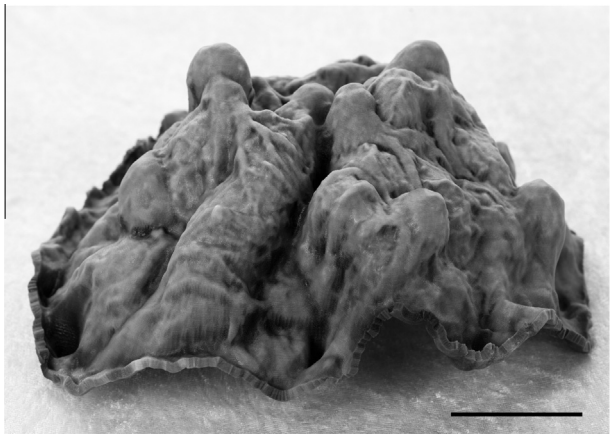

Fig. 7. 3D print. Mesh model transformed into a volume model and printed in 3D. Mesh texture was printed as grayscale. Total glomerulus magnification is approximately 3500×. Scale bar, 5 cm.

surface is too complex, with shaded or too dark areas which the SEM detector cannot capture, 3D reconstruction by photogrammetry is not possible. Flat samples with an almost 2D surface are not suitable either.

The quality of a resulting 3D model is based on several factors, shape, surface structure of the object, the SEM micrograph quality and the software used for 3D reconstruction. The option of 3D printing is of interest, but at present unfortunately linked with a significant reduction in quality.

5. Conclusion and outlook

The study showed that SEM micrographs are suitable for 3D reconstruction by photogrammetry. Our presented method is a simple alternative to generate a 3D surface model of SEM samples. Samples whose surface can be revealed by the detector with overlapping images by rotating around their own axis are advisable for surface reconstruction with optical photogrammetry. Even if this method is not always appropriate, in many cases this transfer of optical photogrammetry seems to be an uncomplicated and useful method also for SEM. Fast and non-destructive generation of 3D surface models is possible. The presented method is a useful extension for SEM research and a significant extension also of teaching. The current resolution of 3D printers is at present still limited but already suited for teaching and it is to be expected that their quality will improve within the near future. For the near future, plans are to automate sample rotation and micrograph acquisition.

Acknowledgments

We thank Prof. Dr. Wolfgang H. Arnold for his expert help in preparing the manuscript and Ms. Christina Wagner for proofreading the manuscript. Finally, we thank two anonymous reviewers for useful comments and suggestions on the manuscript.

Appendix A. Supplementary data

Supplementary data associated with this article can be found, in the online version, at http://dx.doi.org/10.1016/j.jsb.2015.06.010.

References

Bakuła, K., Flasiński, A., 2014. Capabilities of a smartphone for georeferenced 3D model creation: an evaluation. In: 13th International Multidisciplinary Scientific GeoConference SGEM 2013, pp. 85–92.

Barazzetti, L., Forlani, G., Remondino, F., Roncella, R., Scaioni, M., 2011. Experiences and achievements in automated image sequence orientation for close-range photogrammetric projects. In: SPIE Optical Metrology, Vol. 80850F. International Society for Optics and Photonics, pp. 1–13.

Bemis, S.P., Micklethwaite, S., Turner, D., James, M.R., Akciz, S., Thiele, S.T., Bangash, H.A., 2014. Ground-based and UAV-based photogrammetry: a multi-scale, high-resolution mapping tool for structural geology and paleoseismology. J. Struct. Geol. 69 (Part A), 163–178.

Brown, D.C., 1971. Close-Range Camera Calibration. In: Symposium on Close-Range Photogrammetry, pp. 855–866.

Choi, K.S., Lam, E.Y., Wong, K.K.Y., 2006. Source camera identification using footprints from lens aberration. In: Electronic Imaging 2006, Vol. 6069. International Society for Optics and Photonics, pp. 1–8.

Dall'Asta, E., Thoeni, K., Santise, M., Forlani, G., Giacomini, A., Roncella, R., 2015. Network design and quality checks in automatic orientation of close-range photogrammetric blocks. Sensors 15, 7985–8008.

Egerton, R., 2005. Physical Principles of Electron Microscopy: An Introduction to TEM, SEM, and AEM. Springer Science.

Everhart, T.E., Hayes, T.L., 1972. The scanning electron microscope. Sci. Am. 226, 54–69.

Falkingham, P.L., 2012. Acquisition of high resolution three-dimensional models using free, open-source, photogrammetric software. Palaeontol. Electron. 15, 1–15.

Fraser, C.S., Al-Ajlouni, S., 2006. Zoom-dependent camera calibration in digital close-range photogrammetry. Photogram. Eng. Remote Sens. 72, 1017–1026.

Gross, B.C., Erkal, J.L., Lockwood, S.Y., Chen, C., Spence, D.M., 2014. Evaluation of 3D printing and its potential impact on biotechnology and the chemical sciences. Anal. Chem. 86, 3240–3253.

Hoppe, H., DeRose, T., Duchamp, T., McDonald, J., Stuetzle, W., 1992. Surface reconstruction from unorganized points. In: James, J. (Ed.), Proceedings of the 19th Annual Conference on Computer Graphics and Interactive Techniques. Association for Computing Machinery, New York, NY, USA, pp. 71–78 (Thomas Battelle Pacific Northwest Labs, Richland, WA).

Jensen, E.C., 2012. Types of imaging, part 1: electron microscopy. Anat. Rec. 295, 716–721.

Jones, N., 2012. Science in three dimensions: the print revolution. Nature 487, 22–23.

Klein, M., Romero, A., 2007. Evolution of SEM specimen chamber geometries driven by sample and interior characteristics. Microsc. Microanal. 13, 1006–1007.

Lambers, K., Remondino, F., 2008. Optical 3D measurement techniques in archaeology: recent developments and applications. In: Posluschny, A., Lambers, K, Herzog, I. (Eds.), Proceedings of the 35th International Conference on Computer Applications and Quantitative Methods in Archaeology (CAA), pp. 27–35.

Luhmann, T., Robson, S., Kyle, S., Boehm, J., 2013. Close-Range Photogrammetry and 3D Imaging. De Gruyter Textbook. De Gruyter.

Marinello, F., Bariani, P., Savio, E., Horsewell, A., De Chiffre, L., 2008. Critical factors in SEM 3D stereo microscopy. Meas. Sci. Technol. 19, 1–12.

Partridge, R., Conlisk, N., Davies, J.A., 2012. In-lab three-dimensional printing: an inexpensive tool for experimentation and visualization for the field of organogenesis. Organogenesis 8, 22–27.

Reimer, L., 2013. Scanning Electron Microscopy: Physics of Image Formation and Microanalysis. Springer.

Schilling, R., Jastram, B., Wings, O., Schwarz-Wings, D., Issever, A.S., 2014. Reviving the dinosaur: virtual reconstruction and three-dimensional printing of a dinosaur vertebra. Radiology 270, 864–871.

Seligman, A.M., Wasserkrug, H.L., Hanker, J.S., 1966. A new staining method (OTO) for enhancing contrast of lipid-containing membranes and droplets in osmium tetroxide-fixed tissue with osmiophilic thiocarbohydrazide (TCH). J. Cell Biol. 30, 424–432.

Sun, Y., Xia, Y., 2002. Shape-controlled synthesis of gold and silver nanoparticles. Science 298, 2176–2179.

Tesic, J., 2005. Metadata practices for consumer photos. IEEE Multimedia 12, 86–92.

To, T., Nguyen, D., Tran, G., 2015. Automated 3D architecture reconstruction from photogrametric structure and motion: a case study of the "One Pilla" pagoda Hanoi Vietnam. Int. Arch. Photogram. Remote Sens. Spat. Inf. Sci.

Wallace, I.D., Lawson, N.J., Harvey, A.R., Jones, J.D., Moore, A.J., 2005. High-speed close-range photogrammetry for dynamic shape measurement. SPIE Proc. 5580, 358–366.

Yakar, M., Yilmaz, H.M., 2008. Using in volume computing of digital close range photogrammetry. Int. Arch. Photogram. Remote Sens. Spat. Inf. Sci. XXXVII, 119–124.